Information System and Smart City 2023; 3(1): 552.
Original Research Article

Scheduling of integrated biogas energy system for rural areas using improved differential evolutionary algorithm

Tiantian Lv, Yan Gao*

School of Management, University of Shanghai for Science and Technology, Shanghai 200093, China

*** Corresponding author:** Yan Gao, gaoyan@usst.edu.cn

ARTICLE INFO

Received: 18 February 2024
Accepted: 23 February 2024
Available online: 7 April 2024

doi: 10.59400/issc.v3i1.552

ABSTRACT: Due to a lack of rational system design, an enormous amount of energy and resources are wasted or ineffectively utilized in China's rural areas. Therefore, it is crucial to develop a practical energy system that applies to rural areas. In this paper, a Stackelberg game model is established for optimization of integrated energy systems (IES) in rural areas. As a leader, the new energy supplier (NES) develops a price strategy for electricity and heat, and the flexible users and biogas plant (BP) as followers receive price information and make energy consumption plans. Then NES adjusts equipment output based on followers' feedback on energy loads. The objective of our Stackelberg game is to maximize the profit of NES while taking into account the costs of followers. Furthermore, our study designs an improved differential evolutionary algorithm (DEA) to achieve Stackelberg balance. The optimization scheduling result shows that the proposed model can obviously increase the profit of NES by 5.4% and effectively decrease the cost of the biogas plant by 4.5%.

KEYWORDS: integrated biogas energy system; Stackelberg game; improved differential evolutionary algorithm

1. Introduction

1.1. Background

Energy is one of the most important bases for social economy operation. However, the continuous exploitation of energy has led to a rapid decline in fossil energy[1,2]. In order to address the problem of energy shortage, countries are actively researching new energy technologies, especially renewable energy sources such as solar energy, wind energy, and bioenergy[3]. Renewable energy is highly valued around the world due to the abundant resources, wide distribution, and less environmental pollution. Besides, renewable energy has the characteristics of geographical dispersion, discontinuous production, uncontrollability, etc. However, the centralized and unified management of the traditional power network is difficult to adapt to the requirements of large-scale use of renewable energy. Therefore, optimizing the energy system and improving the utility of new energy sources has become a crucial task for researchers and practitioners. Accordingly, integrated energy systems attract wide attention because they combine multiple energy sources and achieve collaborative management of different energies, effectively improving the utility of renewable energy.

Integrated energy system (IES) is an innovative management model composed of multiple energy sources and various types of loads. It can realize the mutual conversion between various energy sources, such as electricity, heat, and natural gas, becoming an important part of the energy system. IES has been

widely studied and developed in recent years; it proves to be adapted to various areas, especially for rural areas. There are abundant types of energy in rural areas, but problems such as poor energy utilization and unreasonable energy structure persist, so it is of great importance to optimize the structure of rural energy system[4,5]. IES model integrates new energy sources that are widely distributed in rural areas into a unified power supplier, improving energy utilization in rural areas.

The operation of IES relies on the synergistic cooperation of multiple stakeholders, and the basic problem to be solved is how to describe the large-scale complex system and the interaction between different stakeholders[6–8]. The Stackelberg game is one of the most important methods to solve the conflict of interests of different market players. It is a two-stage dynamic game with complete information, and the decision-making of the game is sequential. The main idea of the game is that both players choose their own strategies based on each other's possible strategies to ensure maximum benefits. In this game model, the first player to make a decision is called the leader. After the leader, the remaining players make decisions based on the leader's decision, which is called the followers. The leader then adjusts its decision based on the followers' decision until Nash equilibrium is reached[9]. In practical application, how to solve the Stackelberg game and find the optimal results are still challenging problems.

Researchers have spent much effort exploring methods to solve the Stackelberg game. Early Stackelberg games were solved by the classical method, which mainly transforms multiple objective functions into a single objective function. However, the main drawbacks of the classical method are high computational cost and poor convergence, which often fail to obtain the optimal result[10]. In this regard, the differential evolutionary algorithm (DEA) has been developed into a popular option for solving the Stackelberg game. The DEA is a stochastic search algorithm based on population, which is widely used in solving multi-objective optimization problems with high-dimensional data. Each individual in the population of DEA corresponds to a solution vector. The DEA has a unique evolutionary approach; it amplifies the differences between the individuals in the current population to construct a new variant and adopts crossover, mutation, and other operations to enlarge the range of the solution distribution. The DEA starts from a set of initial populations and generates new populations through mutation, where the worse individuals are eliminated and the better ones are retained[11]. After continuous elimination and updating, the optimal solution of the system is searched. However, the traditional DEA is easy to fall into the local optimum, and the algorithm has a long convergence time, which is difficult to meet the increasingly high needs for complex models.

In 2022, China's annual biomass power generation reached 163.7 billion kilowatt hours, accounting for 2% of the total power generation. Among them, biogas power generation had an annual power generation of 3.7 billion kilowatt hours, accounting for 2.3% of biomass power generation[12]. The great development of rural biogas power generation has brought significant economic, social, and ecological benefits. Biogas has the characteristics of wide distribution and diverse sources. Biogas plants (BP) can achieve the resourcefulness of biodegradable waste and improve the utilization rate of energy in rural areas. Currently, biogas plants have been established in many rural areas to improve the utilization of local organic material[13,14]. Biogas plants produce biogas through anaerobic fermentation using a large amount of organic matter from rural areas, and the biogas residue and slurry produced along with the biogas are biochemically processed to make organic fertilizers for sale.

In order to address the above challenges, this paper proposes a Stackelberg game for a rural integrated biogas energy system, which includes a new energy supplier (NES), a biogas plant (BP), and the user. At the same time, this paper designs a new mutation strategy that reduces the possibility of the algorithm falling into the local optimum and accelerates the convergence of the algorithm.

1.2. Literature review

Biogas, which is produced by energy crops or biodegradable wastes, has the advantages of wide distribution and diverse sources. It can meet almost all the demands of rural microgrids; therefore, biogas is usually introduced into rural IES in previous studies. Temperature is a critical factor affecting biogas production, and biogas can be produced at a higher yield under suitable temperature. When the temperature of the biogas digester deviates from optimal, gas production will be significantly reduced. Currently, biogas plants (BP) usually adopt a medium-temperature fermentation process; the internal temperature of the biogas digester is controlled at about 35–40 ℃, which is the most economical temperature range for the operation of biogas digesters. Tan et al.[7] proposed increasing the biogas yield by injecting hot water into the digester; at the same time, a storage tank was set up outside the digester to ensure the reliability of the biogas supply. However, this method did not consider the effect of the uncertainty of ambient temperature on the system. Qin et al.[15] proposed a power supply system with complementary coupling of solar energy and biogas, which generated electricity through solar energy during the daytime and provided a stable power supply with biogas cogeneration in the evening. This system not only effectively reduced the total annual costs and carbon emissions but also improved the efficiency of energy use. In order to illustrate the significance of biogas digesters for energy systems, Wang et al.[16] proposed and established a two-layer optimization model of biogas integrated energy systems with natural gas price fluctuation, which improved the thermal comfort and energy efficiency of heat users. The above literatures demonstrate the operating conditions and important value of biogas digesters.

With the development of energy markets, the behavior of users is gradually taken into account in the energy management of IES. In the energy trading process, the energy supplier prioritizes the price strategy based on the predicted load demand, and users adjust their energy consumption behavior based on the price information[17]. The Stackelberg game can effectively describe this kind of interactive behavior of IES. Huang et al.[18] proposed a two-stage energy management method of heat-electricity IES considering dynamic pricing based on the Stackelberg game. The model markedly enhanced renewable energy utilization and reduced the cost of both energy supplies and users. The Stackelberg game model can also be used for energy interconnection systems of multiple objectives. Li et al.[19] established a Stackelberg game optimization model for distributed integrated energy systems with hierarchical zoning, which fully considered the interaction of energy and interests between different communities. Wang et al.[20] proposed a model for optimal scheduling of electrical and thermal integrated energy systems based on the Stackelberg game, which aimed at maximizing the revenue of energy suppliers.

Evolutionary algorithms are one of the most important methods for solving Stackelberg games, and in recent years much more studies have focused on the optimization and improvement of evolutionary algorithms. Traditional evolutionary algorithms are prone to fall into local optimal solutions when facing complex optimization problems due to insufficient population diversity and single variance vectors. In order to solve this problem, Jiang et al.[10] optimized the mutation strategy and increased the population diversity. They introduced a self-adaptive operator to ensure the diversity of the mutation strategy and reduce the probability of the algorithm falling into local optimal results. Youssef et al.[11] proposed an optimal stochastic mutation strategy, mutating certain genes of the optimal chromosome within the search range. The strategy provided the algorithm with a stronger exploration capability at a later stage of evolution in order to improve the ability to jump out of the local optimum. Zhang et al.[21], on the other hand, designed a collaborative initialization strategy to generate high-quality initial bi-populations to accelerate the evolutionary process, and they designed problem-specific evolutionary operators for each sub-population. This dual-cooperative model, which shares advantageous information among different

populations, accelerated the convergence of the algorithm.

1.3. Work in the paper

A Stackelberg game model is established in this paper for optimization of integrated energy systems (IES) in rural areas. The industrial user-biogas plant is first introduced into Stackelberg game-based IES and plays a critical role as a market player. Moreover, we present a novel DEA for solving the Stackelberg game, addressing the challenges faced by traditional algorithms. Our work is detailly described and listed as follows:

(1) For the first time, industrial users are introduced into Stackelberg game-based IES. The processes in biogas plants are divided and transferred into different kinds of flexible loads, allowing industrial users to participate in games, which makes the model more practical and usable.

(2) The Stackelberg game-based IES is solved by an improved differential evolutionary algorithm (DEA) in our study. The DE/rand2 strategy and the DE/best2 strategy are coupled into a composite mutation strategy to give our algorithm strong global-search ability in the early stage of iteration and better local-search performance at later times.

In summary, the model proposed in this paper improves the accuracy and availability of energy scheduling in rural areas and provides a promising solving method for Stackelberg game-based IES.

2. Mathematical model

2.1. Structure of IES

Figure 1 illustrates the structure of our integrated energy system (IES). The electricity in our IES mainly comes from a new energy supplier (NES), of which wind turbines (WT), photovoltaic panels (PV), combined heat and power (CHP), and energy storage systems (ESS) are included. The equipment of the biogas plant (BP) consists of biogas digesters, gas boilers (GB), solar collectors (SC), thermal storage tanks (TST), and other digesters. Among this equipment, solar collectors generate heat by absorbing solar energy, gas boilers consume biogas to produce heat, and the digesters are kept warm by the water circulation from thermal storage tanks. Biogas residual and biogas slurry are regularly extracted from biogas digesters to produce green organic fertilizer and liquid fertilizer, which continuously creates revenue for BP. For the common user, flexible loads are introduced to decrease energy costs and reduce fluctuation of electrical loads. Moreover, the rural electricity and heat grid are additionally added in order to maintain the balance of electricity and heat in our IES.

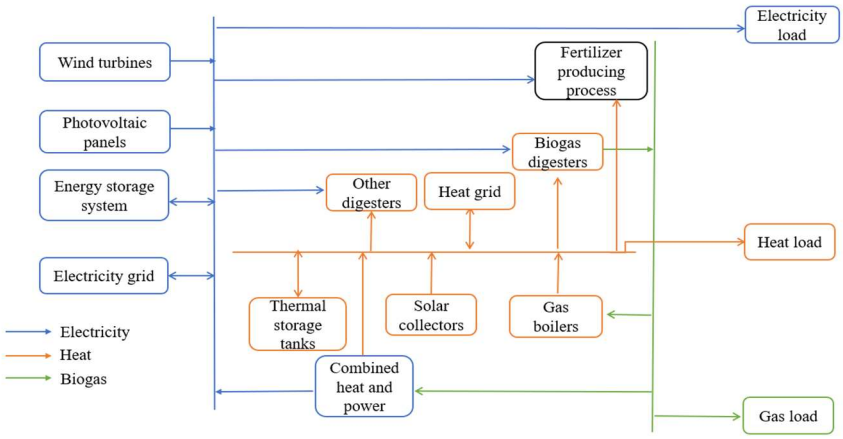

Figure 1. Structure of the introduced IES.

2.2. Framework of the Stackelberg game

A Stackelberg game is constructed to describe the rural IES where the participants deeply interact with each other, and an optimal result is eventually achieved through the game. NES, as the leader of the game model, prices energy and adjusts equipment output based on the load demand of followers. The objective of NES is to maximize its profit, which is the revenue from energy sales minus the operation costs of equipment. The objective of BP is also to maximize the profit, which is mainly realized by optimizing load distribution because of the high rate of energy cost in its total costs. The strategies of BP are as follows: 1) Adjust the output of the biogas boiler based on the time-of-use heat price. 2) Optimize the flexible load in different periods to decrease power costs on the premise of normally producing biogas and fertilizer. The user aims at maximizing its customer surplus by co-optimizing consumer satisfaction index (CSI) and flexible load. The structure and interconnection of our game are shown in **Figure 2**.

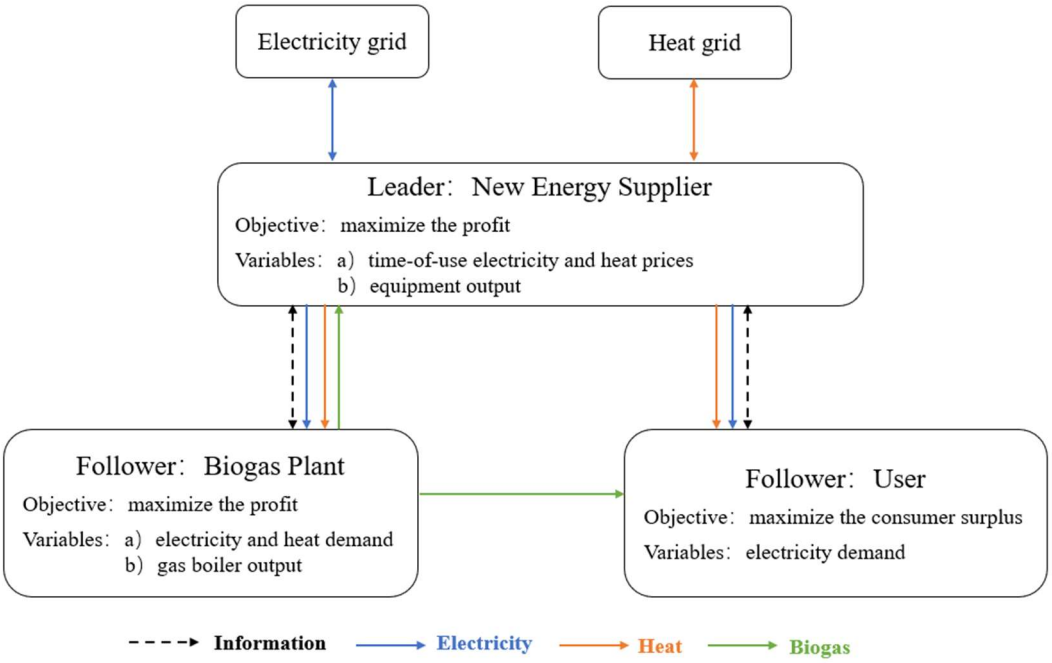

Figure 2. Framework of Stackelberg game.

Stage 1: The NES first sets the electricity price and heat price for residential and industrial users, respectively. The price information is then transmitted to followers.

Stage 2: BP and the user determine the energy consumption plants based on the price information from NES, so the optimal decision of the followers can be regarded as a function of the decision variables of the leader.

Through the above description, we can find that the strategy of BP and the user are established on the pricing of NES, and their optimization results will in turn affect the pricing of NES. This kind of energy transaction process is in line with the situation of the Stackelberg game and can be expressed as follows:

$$G = \{N; \rho_{NES}; \{\delta_{BP}, \ \delta_{user}\}; F_{NES}, \{F_{BP}, \ F_{user}\}\} \tag{1}$$

where N is the number of participants, ρ_{NES} is the price strategy set by NES; δ_{BP} is the load demand of BP; δ_{user} is the load demand of the user; F_{NES} is the revenue of NES; F_{BP} is the revenue of the biogas plant; F_{user} is the consumer surplus of the user.

The game reaches Stackelberg equilibrium when all followers make optimal responses according to the leader's strategy and the leader accepts this response. If $(\rho^*_{\text{NES}}, \delta^*_{\text{BP}}, \delta^*_{\text{users}})$ is the equilibrium solution of our game, it needs to satisfy:

$$\begin{cases} F_{\text{NES}}(\rho^*_{\text{NES}}, \delta^*_{\text{BP}}, \delta^*_{\text{user}}) \geq F_{\text{NES}}(\rho_{\text{NES}}, \delta^*_{\text{BP}}, \delta^*_{\text{user}}) \\ F_{\text{BP}}(\rho^*_{\text{NES}}, \delta^*_{\text{BP}}, \delta^*_{\text{user}}) \geq F_{\text{NES}}(\rho^*_{\text{NES}}, \delta_{\text{BP}}, \delta^*_{\text{user}}) \\ F_{\text{user}}(\rho^*_{\text{NES}}, \delta^*_{\text{BP}}, \delta^*_{\text{user}}) \geq F_{\text{NES}}(\rho^*_{\text{NES}}, \delta^*_{\text{BP}}, \delta_{\text{user}}) \end{cases} \tag{2}$$

Under this situation the Stackelberg game-based IES achieves balance.

2.3. Description of the new energy suppliers (NES)

2.3.1. Objective function of the NES

The NES develops price strategy for energy and provides energy by operation of WT, PV, CHP and ESS. The objective function of NES is as follow:

$$F_{\text{NES}} = F_{\text{NES-r}} - F_{\text{NES-c}} - F_{\text{NES-o}} + I_{\text{net},t} \tag{3}$$

$$F_{\text{NES-r}} = \sum_{t=1}^{T} (I_{\text{sell-BP},t} + I_{\text{sell-user},t}) \tag{4}$$

$$F_{\text{NES-c}} = \sum_{t=1}^{T} (G_{\text{CHP},t} c_{\text{gas},t}) \tag{5}$$

$$F_{\text{NES-o}} = \sum_{t=1}^{T} (C_{\text{CHP},t} + C_{\text{ESS},t} + C_{\text{WT},t} + C_{\text{PV},t}) \tag{6}$$

$$I_{\text{net},t} = \sum_{t=1}^{T} (p_{\text{buy},t} P_{\text{buy,t}} + p_{\text{sell},t} P_{\text{sell,t}}) \tag{7}$$

The following equations show the energy sold to biogas plants and users by energy suppliers, as well as the cost of each item:

$$I_{\text{sell-BP},t} = (P_{\text{BP},t} c^e_{\text{BP},t} + H_{\text{BP},t} c^h_{\text{BP},t}) \triangle t \tag{8}$$

$$I_{\text{sell-user},t} = (P_{\text{user},t} c^e_{\text{user},t} + H_{\text{user},t} c^h_{\text{user},t}) \triangle t \tag{9}$$

$$C_{\text{device},t} = \sum a_{\text{device}} P_{\text{device},t} \tag{10}$$

where, device = WT, PV, CHP, ESS.

2.3.2. Constraints of the NES

(1) Electricity balance constraint

When NES provides electricity to BP and the user, the electricity balance in IES model should satisfy the below equation:

$$P_{\text{e-net},t} + P_{\text{WT},t} + P_{\text{PV},t} + P_{\text{CHP},t} = P_{\text{user},t} + P_{\text{BP},t} + P^{ch}_{\text{ESS},t} - P^{dis}_{\text{ESS},t} \tag{11}$$

(2) Heat balance constraint

The constraint of heat balance is as follow:

$$H_{\mathrm{CHP},t} = H_{\mathrm{user},t} + H_{\mathrm{BP},t} + H_{\mathrm{net},t} \tag{12}$$

(3) Equipment constraint

Wind turbines (WT): Wind turbines are devices that convert the kinetic energy of wind to electrical energy. As a kind of clean renewable energy, wind energy has been paid much more attention by all countries in the world. The output power of WT can be calculated by the following equation[22]:

$$P_{\mathrm{WT},t} = \begin{cases} 0 & v < v_{\mathrm{cut,i}}, v > v_{\mathrm{cut,o}} \\ \dfrac{v_{\mathrm{actual}} - v_{\mathrm{cut,i}}}{v_{\mathrm{rated}} - v_{\mathrm{cut,i}}} P_{\mathrm{WT}}^{\mathrm{rated}} N_{\mathrm{WT}} & v_{\mathrm{cut,i}} \le v < v_{\mathrm{rated}} \\ P_{\mathrm{WT}}^{\mathrm{rated}} N_{\mathrm{WT}} & v_{\mathrm{rated}} \le v < v_{\mathrm{cut,o}} \end{cases} \tag{13}$$

where V_{actual} is the actual wind speed; V_{rated} is the rated wind speed; $P_{\mathrm{WT}}^{\mathrm{rated}}$ is the rated output power; N_{WT} is the number of wind turbines.

Photovoltaic panels (PV): PV can directly convert the solar energy to electrical energy through the photovoltaic effect of semiconductors. The cost of PV power has decreased markedly in recent years, which leads to a boom of PV installation in the whole world. The output power of PV can be calculated by the following equation[23]:

$$P_{\mathrm{PV},t} = P_{\mathrm{PV}}^{\mathrm{rated}} (G_{\mathrm{w}} / G_{\mathrm{PV}}^{\mathrm{std}})(1 - \eta_{\mathrm{PV}}^{\mathrm{T}} (T_{\mathrm{b}} - T_{\mathrm{PV}}^{\mathrm{ref}}))N_{\mathrm{PV}} \tag{14}$$

where $P_{\mathrm{PV}}^{\mathrm{rated}}$ is the rated output power of PV, G_{W} is the radiation intensity at the working point; $G_{\mathrm{PV}}^{\mathrm{std}}$ is the standard radiation intensity; $\eta_{\mathrm{PV}}^{\mathrm{T}}$ is the power temperature coefficient; T_{b} is the cell temperature at the working point; $T_{\mathrm{PV}}^{\mathrm{ref}}$ is the reference temperature; N_{PV} is the number of PV.

Combined heat and power (CHP): CHP is biogas-fueled equipment through which the high-level heat energy generated from the combustion of biogas is converted to electricity and low-level heat energy is collected through a waste heat boiler (WHB)[24]. In this system, CHP mainly consumes biogas to output electrical power and heat for followers:

$$P_{\mathrm{CHP},t}^{\mathrm{e}} = \eta_{\mathrm{CHP}}^{\mathrm{e}} P_{\mathrm{CHP},t}^{\mathrm{g}} \tag{15}$$

$$P_{\mathrm{CHP},t}^{\mathrm{h}} = \partial P_{\mathrm{CHP},t}^{\mathrm{e}} \tag{16}$$

$$0 \le P_{\mathrm{CHP},t}^{\mathrm{e}} \le P_{\mathrm{CHP,max}}^{\mathrm{e}} \tag{17}$$

$$-\Delta P_{\mathrm{di}} \le P_{\mathrm{i},t} - P_{\mathrm{i},t-1} \le \Delta P_{\mathrm{ui}} \tag{18}$$

where $\eta_{\mathrm{CHP,t}}^{\mathrm{e}}$ is the electricity generating efficiency of CHP; ∂ is the heat-electricity generation ratio of the CHP; ΔP_{di}, ΔP_{ui} are the upper and lower limits of the CHP ramp rate.

Energy storage system (ESS): ESS is introduced to store excess power and release it when needed, which achieves efficient use of new energy power. The capacity constraint of ESS is shown[25] in equation:

$$E_{\mathrm{ESS}}^{(t)} = E_{\mathrm{ESS}}^{(t-1)} (1 - \sigma) + \eta_{\mathrm{ESS}} P_{\mathrm{ESS}}^{(t)} \Delta t \tag{19}$$

where σ denotes the energy loss coefficient of ESS; η_{ESS} represents charging and discharging efficiency of ESS; and Δt denotes the time interval.

The storage capacity of ESS is constrained by the below equations:

$$S_{\min}E_{\max} \le E_t \le S_{\max}E_{\max} \tag{20}$$

$$E_0 = S_0E_{\max} \tag{21}$$

where $E_{\max}$ is the maximum capacity of ESS; $S_{\max}$, $S_{\min}$ are the maximum and minimum storage coefficients of ESS, here $S_{\max}$ is 0.9, $S_{\min}$ is 0.1; E_0 is the electric power stored by ESS at initial time; S_0 is the storage coefficient of ESS at initial time[17].

The charging and discharging power constraints of ESS are shown in Equations (22)–(24). Because of the restriction of charging and discharging power, the electric power of ESS at time t and $t-1$ is constrained by Equation (25):

$$0 \le P_{\mathrm{ch},t} \le u_{\mathrm{ch},t}P_{\max,t} \tag{22}$$

$$0 \le P_{\mathrm{dc},t} \le u_{\mathrm{dc},t}P_{\max,t} \tag{23}$$

$$0 \le u_{\mathrm{ch},t} + u_{\mathrm{dc},t} \le 1 \tag{24}$$

$$-\Delta E_{\mathrm{di}} \le E_{\mathrm{i},t} - E_{\mathrm{i},t-1} \le \Delta E_{\mathrm{ui}} \tag{25}$$

where $u_{\mathrm{ch},t}$ and $u_{\mathrm{dc},t}$ are the charging and discharging power states of ESS, taking the value of 0 or 1; ΔE_{di} and ΔE_{ui} are the maximum downward and upward climbing rates of ESS, respectively.

2.4. Description of biogas plant (BP)

2.4.1. Objective function of the BP

The BP obtains revenue from selling biogas and fertilizer, meantime it adjusts energy consumption distribution based on electricity price set by NES. The objective function of BP is shown below:

$$F_{\mathrm{BP}} = F_{\mathrm{BP\text{-}r}} - F_{\mathrm{BP\text{-}c}} - F_{\mathrm{BP\text{-}o}} \tag{26}$$

$$F_{\mathrm{BP\text{-}r}} = \sum_{t=1}^{T}(I^{\mathrm{g}}_{\mathrm{sell},t} + I^{\mathrm{OF}}_{\mathrm{sell},t}) \tag{27}$$

$$F_{\mathrm{BP\text{-}c}} = \sum_{t=1}^{T}(C_{\mathrm{e},t} + C_{\mathrm{h},t}) \tag{28}$$

$$F_{\mathrm{BP\text{-}o}} = \sum_{t=1}^{T}(C_{\mathrm{SC},t} + C_{\mathrm{GB},t}) \tag{29}$$

2.4.2. Constraints of the BP

(1) Process of biogas plant

The process of biogas plants is illustrated in **Figure 3**. The biogas plant produces biogas through the fermentation process in biogas digesters and regularly extracts biogas slurry and residue to prepare organic fertilizer. Based on the process characteristics, electrical loads in BP can be divided into fixed electrical loads and shiftable electrical loads. The electrical loads of digesters are fixed loads because biomass in digesters needs to be stirred continuously to ensure mixing evenly. The solid-liquid separation process of biogas residue and the crushing process of organic fertilizer usually run for a few hours, and these processes cannot be divided into sections; therefore, they are shiftable electrical loads.

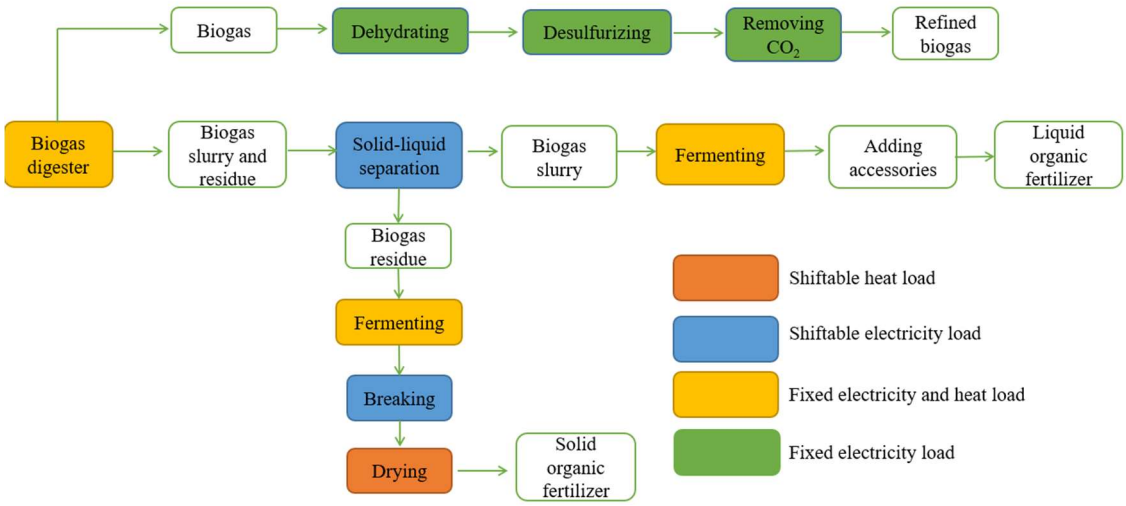

Figure 3. Internal process of biogas plant.

The electrical loads in BP should satisfy the following constraints:

$$P_{\mathrm{BP},t} = P_{\mathrm{BP,fix}} + P_{\mathrm{BP,shift1}} + P_{\mathrm{BP,shift2}} \tag{30}$$

Let the shiftable period of crushing process be $[t_{\mathrm{shift1}-}, t_{\mathrm{shift1}+}]$, and let the shiftable period of solid-liquid separation process be $[t_{\mathrm{shift2}-}, t_{\mathrm{shift2}+}]$. The constraints of below equations should be satisfied[26].

$$\sum_{t=\tau_1}^{\tau_1+t_{\mathrm{shift1}}-1} y_{h1} = t_{\mathrm{shift1}} \tag{31}$$

$$\sum_{t=\tau_2}^{\tau_2+t_{\mathrm{shift2}}-1} y_{h2} = t_{\mathrm{shift2}} \tag{32}$$

Heat loads in BP are divided into fixed loads and shiftable loads. The fermentation process belongs to fixed heat load because the digesters need to be kept warm to maintain the fermentation rate at all times. The drying process of fertilizer usually lasts for several hours; it is a continuous process that cannot be divided into segments. Therefore, based on rational decision, BP arranges the drying process at a time period when the heat price is relatively low. The heat loads in BP should satisfy the following constraints:

$$H_{\mathrm{load}} = H_{\mathrm{BP}}^{\mathrm{fix}} + H_{\mathrm{BP}}^{\mathrm{shift}} \tag{33}$$

Let the operating period of the shiftable heat load be $[h_{\mathrm{shift}-}, h_{\mathrm{shift}+}]$, and let the constraint is described as equation when the load is shifted into the time period with τ as the starting time:

$$\sum_{t=\tau}^{\tau+h_{\mathrm{shift}}-1} y_h = h_{\mathrm{shift}} \tag{34}$$

where h_{shift} is the total operating hours of drying process, y_h is a state variable that determines whether the load is shifted or not, and takes the value of 0 or 1, $y_h = 0$ denotes the load is not shifted.

(2) Heat balance constraint

The thermal model of a biogas plant is illustrated in **Figure 4**. The drying temperature of fertilizer is usually in the range of 60~80 ℃, and it is difficult for a thermal storage tank (TST) to reach this temperature through circulating water, so the required heat for the drying process is provided by CHP and GB. While the internal temperature of digesters is usually controlled at about 40 ℃, the use of TST

for heat retention can not only reduce temperature fluctuation in digesters but also decrease heat loss in the heat transfer process.

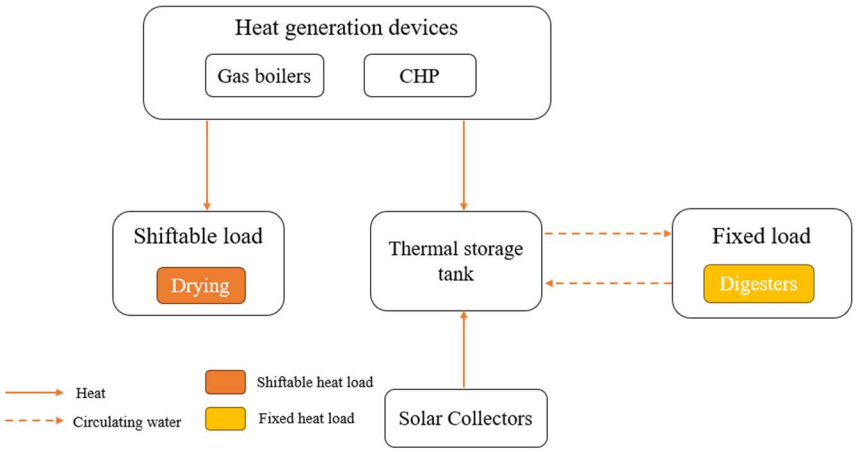

Figure 4. Illustration of thermal model of biogas plant.

The equations of heat balance of TST are as follows:

$$H_{\mathrm{GB},t}^{\mathrm{fix}} + H_{\mathrm{CHP},t}^{\mathrm{fix}} + H_{\mathrm{SC},t} - H_{\mathrm{loss},t} = H_{\mathrm{tank},t} \tag{35}$$

$$H_{\mathrm{loss}} = H_{\mathrm{tank-loss}} + H_{\mathrm{wa\text{-}loss}} \tag{36}$$

$$H_{\mathrm{GB},t} = H_{\mathrm{GB},t}^{\mathrm{fix}} + H_{\mathrm{GB},t}^{\mathrm{sft}} \tag{37}$$

$$H_{\mathrm{buy},t} = H_{\mathrm{CHP},t}^{\mathrm{fix}} + H_{\mathrm{CHP},t}^{\mathrm{sft}} \tag{38}$$

$$H_{\mathrm{BP}}^{\mathrm{fix}} = (H_{\mathrm{out}} - H_{\mathrm{in}})\eta_{\mathrm{BP}} \tag{39}$$

where η_{BP} is the heat transfer loss coefficient of the pipeline in BP, which is mainly determined by the material of the pipeline, heat transfer areas and fluid temperature.

(3) Equipment constraints

Biogas digester:

Biogas digesters produce refined biogas for CHP to generate electricity and for the user's daily needs. The internal temperature of the biogas digester is an important factor affecting biogas production, so it is necessary to keep the temperature in an optimal range. In our model, a thermal storage tank (TST) is applied to maintain the temperature of digesters through circulating water, which guarantees the continuous and efficient production of biogas.

The biogas produced from digesters contains about 30 percent carbon dioxide and less than 1 percent sulfide. The high content of carbon dioxide will affect the combustion of biogas; moreover, the sulfide is able to cause corrosion of the equipment. Therefore, desulphurization and decarbonization are required to obtain usable biogas.

If considering the daily biomass in IES a constant value and ignoring the effect of the concentration of biomass waste, the daily biogas production can be calculated by equation:

$$G_{\mathrm{BP}} = \gamma_m m \tag{40}$$

where γ_m is the gas production rate of biogas digesters and m is the daily mass of biomass in IES. Among

them, γ_m is mainly related to the internal temperature of digesters when fermentation raw materials and bacteria remain basically unchanged. When the temperature in digesters remains stable, γ_m is nearly a constant value, and the biogas production is uniformly distributed throughout the day.

Organic fertilizer production process:

Biogas is a kind of promising green energy without doubt, but production of biogas is always accompanied by the generation of biogas residue and slurry. Nowadays, biogas residue and slurry are proved to be able to be applied for producing organic fertilizer.

Through the solid-liquid separation, biogas residue is separated and further transformed into solid organic fertilizer through a series of processes, including fermentation, crushing, and drying. After fermentation of biogas slurry, the liquid organic fertilizer is obtained by adding auxiliary materials. The fermentation process is similar to that of biogas digesters, which requires continuous stirring and optimal temperature. The production volume of fertilizer is deduced from the conservation of mass as shown in equation:

$$G_{\mathrm{OF}} = (\rho_m m - \rho_{\mathrm{gas}} G_{\mathrm{BP}}) \times R_{\mathrm{OF}} \tag{41}$$

$$P_{\mathrm{OF}} = \rho_{\mathrm{OF}} G_{\mathrm{OF}} \tag{42}$$

where ρ_m is the density of biomass, ρ_{gas} is the density of biogas, and ρ_{OF} is the electricity consumption for producing a kilogram of fertilizer.

Solar collector (SC):

A solar collector is a device that converts the solar energy into heat energy. Generally, it consists of a concentrator and a receiver to complete the heat transfer process. The efficiency of SC can be calculated by the following equation:

$$\eta_{\mathrm{SC}} = \frac{m c_{\mathrm{p}} (T_{\mathrm{out}} - T_{\mathrm{in}})}{A G_{\mathrm{T}}} \tag{43}$$

where m is the mass flow rate of the fluid flowing through the collector, c_{p} is the specific heat capacity of the fluid, T_{in} and T_{out} are the average fluid inlet and outlet temperatures, A is the collector area of SC, G_{T} is the solar flux received by SC, and η_{SC} is the efficiency of SC.

Biogas boiler (GB):

A biogas boiler is heat production equipment with high thermal efficiency in IES. BP will increase the output of GB when the operating cost of GB is lower than the heat price set by NES. The heat produced by GB is partly supplied to fixed heat loads and partly to shiftable heat loads. The power of GB is constrained by the following equation:

$$H_{\mathrm{GB},t} = \eta_{\mathrm{GB,h}} G_{\mathrm{GB},t} \tag{44}$$

$$0 \le H_{\mathrm{GB},t} \le H_{\mathrm{GB,max}} \tag{45}$$

$$-\Delta H_{\mathrm{di}} \le H_{\mathrm{GB},t} - H_{\mathrm{GB},t-1} \le \Delta H_{\mathrm{ui}} \tag{46}$$

where $\eta_{\mathrm{GB,h}}$ is the heat production efficiency of the GB, and $H_{\mathrm{GB,max}}$ is the rated power of the GB. ΔH_{di}, ΔH_{ui} are the maximum upward and downward climbing rates of GB, respectively.

Thermal storage tanks (TST):

A thermal storage tank is the equipment being able to store heat energy by raising the temperature of the storage water. The TST is used to maintain the temperature of digesters in BP, which has the advantages of accurate temperature control, small temperature fluctuation, and low heat loss. In the operation of BP, the solar collectors and biogas boilers provide heat for TST, and TST transfers heat to digesters through the circulating water. The heat balance of TST is constrained by the following equation:

$$H_{\mathrm{GB},t}^{\mathrm{fix}} + H_{\mathrm{CHP},t}^{\mathrm{fix}} + H_{\mathrm{SC},t} - H_{\mathrm{tank\text{-}loss},t} = H_{\mathrm{tank},t} \tag{47}$$

$$H_{\mathrm{tank\text{-}loss}} = a_1(T_{\mathrm{wa}} - T_0) \tag{48}$$

$$H_{\mathrm{wa\text{-}loss}} = H_{\mathrm{BP}}^{\mathrm{fix}} / (1 - a_2) \tag{49}$$

where H_{loss} is the heat loss of TST; T_{wa} is the temperature of the storage tank at different times; T_0 is the ambient temperature; a_1 is the coefficient of heat loss; it is closely related to the heat exchange area, material of TST, and so on. a_2 is the heat loss in heat transfer lines.

2.5. Description of the user

2.5.1. Objective function of the user

The flexible user purchases electricity and heat energy from NES and consumes biogas in daily life. The objective function of the user is maximizing the consumer benefit, which is the consumer satisfaction index (CSI) minus the energy costs[27]. The objective function of the user is shown in Equation (51), and CSI and energy costs can be calculated by Equations (52) and (53):

$$F_{\mathrm{user}} = U - F_{\mathrm{user\text{-}c}} \tag{51}$$

$$U(x,w) = \begin{cases} \omega x - \dfrac{\sigma}{2}x^2, 0 \le x \le \dfrac{\omega}{\sigma} \\ \dfrac{\omega^2}{2\sigma}, x > \dfrac{\omega}{\sigma} \end{cases} \tag{52}$$

$$F_{\mathrm{user\text{-}c}} = \sum_{t=1}^{T} (I_{\mathrm{buy},t}^{\mathrm{e}} + I_{\mathrm{buy},t}^{\mathrm{h}} + I_{\mathrm{buy},t}^{\mathrm{g}}) \tag{53}$$

where ω is the parameter representing the user's preference, which may take different values at different times of the day, σ is the predetermined parameter, and it takes the value in the range of (0, 1] and x is the amount of energy consumed by the user.

2.5.2. Constraints of the user

The electrical loads of the user are divided into fixed loads and transferable loads. The constraints of the electrical load of the user are shown as follows:

$$P_{\mathrm{load}} = P_{\mathrm{fix}} + P_{\mathrm{trans}} \tag{54}$$

The transferable load represents a kind of load that can be transferred to a certain period of time, but the total load power before and after the transfer should keep the same. Let the time period of the transferable load be $[t_{\mathrm{trans}}^{-}, t_{\mathrm{trans}}^{+}]$ and the minimum transfer duration be $T_{\mathrm{trans}}^{\min}$. The constraints on the transferable load and the minimum continuous operation time are shown in Equations (55) and (56):

$$zP_{\mathrm{trans}}^{\min} \leqslant P_{\mathrm{trans}} \leqslant zP_{\mathrm{trans}}^{\max} \tag{55}$$

$$\sum_{\tau=t}^{t+T_{\text{trans}}^{\min}-1} z \geq T_{\text{trans}}^{\min} \tag{56}$$

where $P_{\text{trans}}^{\min}$ $P_{\text{trans}}^{\max}$ are the minimum and maximum power values set for transferable load; z takes 0 to indicate that the load is not transferred, and 1 to indicate that the load is transferred.

2.6. Differential evolutionary algorithms (DEA)

A Stackelberg game model is constructed with three participants in this study. Each of the participants provides energy or information for others and optimizes their objective functions based on information they received. For these multi-objective optimization problems of large-scale multidimensional nonlinear systems, the traditional optimization algorithm—mixed-integer linear programming (MILP)—is no longer suitable and difficult to solve, so we adopt the improved differential evolutionary algorithm (DEA) to solve the problem. The improved DEA introduced in this paper has the advantages of easy implementation and high computational efficiency[28]. The flowchart of the algorithm steps is shown in **Figure 5**. The improvements of DEA in this paper are listed as below.

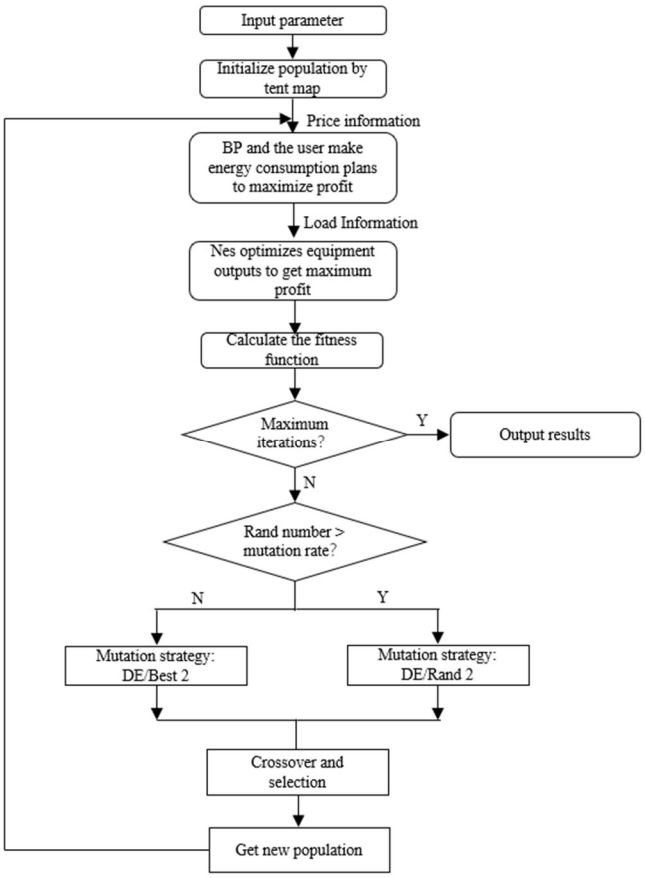

Figure 5. Flowchart of improved differential evolutionary algorithm.

(1) Generation of initial population

The random generation of the initial population for traditional difference algorithms may lead to a long convergence time for the algorithm. To overcome these drawbacks, this paper uses tent mapping to generate the initial population. The generated initial population, distributed uniformly in the value range,

effectively reduces the convergence time. The method of tent mapping is shown in equation:

$$Z_{j,k+1} = \begin{cases} \dfrac{Z_{j,k}}{\beta}, Z_{j,k} \in (0, \beta] \\ \dfrac{1 - Z_{j,k}}{1 - \beta}, Z_{j,k} \in (\beta, 1] \end{cases} \tag{57}$$

where β is the control variable whose value range is (0, 1), and here β takes the value 1/2.

(2) Mutation strategy

Among the mutation strategies of traditional difference algorithms, the DE/rand1 and DE/rand2 strategies have excellent global search performance but lack the memory for local better solutions. The DE/Best1 and DE/Best2 strategies have better local optimization performance but poor global-searching ability, which usually leads the algorithm into local optimum. For this reason, we introduce the exponential mutation rate (MR) that varies in the iteration process:

$$\mathrm{MR} = \mathrm{MR}_{\min} * (\mathrm{MR}_{\max} / \mathrm{MR}_{\min})^{(\mathrm{iter}/\mathrm{itermax})} \tag{58}$$

When the random number is not larger than *MR*, the DE/Best2 strategy is executed, when the random number is larger than MR, the DE/Rand2 strategy is executed.

In the initial stages of iteration, the value of MR is quite small, and the algorithm mainly performs DE/Rand2 strategy, avoiding the algorithm falling into local optimum in the early stage. As the iteration process proceeds, the value of MR gradually increases, leading to the growing probability of executing the DE/Best2 strategy. This kind of composite strategy provides the algorithm with better global-searching ability in the early stage and excellent local-searching performance at a later time.

(3) Fitness function

Most of the fitness functions of traditional differential algorithms are single objective functions. They only consider the benefits of the leader in the Stackelberg game and do not take into account the interests of other participants. However, in this paper the fitness function is constructed by the leader's profit and the follower's energy cost, which ensures the multiple interests in the Stackelberg game. The fitness function is shown in the following equation:

$$F_t = 0.5 * F_{\mathrm{NES}} - 0.3 * F_{\mathrm{BP\text{-}c}} - 0.2 * F_{\mathrm{user\text{-}c}} \tag{59}$$

The steps of the algorithm are as follows:

1) Set the population size and basic parameters of the algorithm.
2) Generate initial populations through tent mapping.
3) NES transmits information about the initial population to BP and the user.
4) BP and the user optimize their energy consumption plans and equipment output based on the information they received, aiming at maximizing the total profit (or consumer surplus). Thus, the operation condition of equipment and load distribution at different times are obtained, and then the information is transferred to NES.
5) NES adjusts the output of the equipment based on the load distribution of followers. First of all, NES should keep the energy balance of the system and guarantee the energy demand is met at all periods. On this premise, NES further optimizes the operation condition of equipment to save its total costs.
6) Calculate the fitness function, output, and record the best individual whose fitness value is the

largest.

7) The new population with higher fitness is generated through the processes of mutation, crossover, and selection. The mutation strategy is the composite strategy introduced above.
8) Repeat the process until equilibrium.

3. Simulation and analysis

3.1. Parameter setting

An actual rural IES in south China is selected as the test system to verify the effectiveness of the model we proposed. The IES consists of a variety of distributed new energy sources, and they are fully utilized by PV, WT, CHP, SC, and other energy conversion devices. The economic and technical parameters of devices in our IES are shown in **Table 1**. The parameters of flexible loads of BP and the user are shown in **Table 2**. The time-of-use prices of energy from the grid at different times are listed in **Table 3**. Electricity and heat price of the grid at different times are shown in **Table 4**.

Table 1. Economic and technical parameters of the equipment.

Equipment	Technical parameters	Operation and maintenance cost/￥10,000
Wind turbine	-	0.10
Photovoltaic panel	η = 0.004	0.10
Combined heat and power	η = 0.3, φ = 2.1	0.20
Energy storage system	σ = 0.01, η = 0.98, S_{max} = 0.9, S_{min} = 0.1	0.10
Biogas digester	γ = 0.30 m^3/kg	0.05
Solar collector	η = 0.30	0.10
Biogas boiler	η = 0.95	0.10
Thermal storage tanks	$a1$ = 10, $a2$ = 0.02, η_{BP} = 0.98	0.02

Table 2. Flexible load parameters.

Flexible load	Parameters
Shiftable electrical load-1	$[t_{shift1-}, t_{shift1+}]$=[5, 22]; t_s=3 h
Shiftable electrical load-2	$[t_{shift2-}, t_{shift2+}]$=[5, 22]; t_s=2 h;
Shiftable heat load	$[h_{shift-}, h_{shift+}]$=[5, 22]; h_s=3 h;
Transferable electrical load	$[t_{trans}^{-}, t_{trans}^{+}]$=[5, 22]; T_{min}^{tran}=2 h; $[P_{min}^{trans}, P_{max}^{trans}]$=[8, 26.7]

Table 3. Pricing strategy of NES at different time.

Time period		Price range
Industrial electricity price	Peak time	[0.63, 2.40]
	Flat time	[0.42, 1.60]
	Valley time	[0.21, 1.20]
Residential electricity price	Peak time	[0.60, 1.20]
	Flat time	[0.40, 0.80]
	Valley time	[0.20, 0.60]
Heat price	Peak time	[0.60, 1.20]
	Flat time	[0.40, 0.80]
	Valley time	[0.30, 0.60]

Table 4. Electricity and heat price of grid at different times.

Time period		Price
Electricity sell price	Peak time	1.2
	Flat time	0.8
	Valley time	0.6
Electricity purchase price	Peak time	0.6
	Flat time	0.4
	Valley time	0.2
Heat sell price	Peak time	0.6
	Flat time	0.4
	Valley time	0.3
Heat purchase price	Peak time	1.2
	Flat time	0.8
	Valley time	0.6

3.2. Experimental analysis

The pricing strategies of NES for the initial price and optimized price of electricity are shown in the figure above. The upper limit of energy price is the sale electricity price of grid, and the lower limit is the purchase electricity price of grid. **Figures 6** and **7** show the time of use price of residential electricity, industrial electricity price, and heat energy, respectively. It can be easily found that there is an obvious difference between the optimal price and initial price, which indicates that the improved DEA effectively optimizes the decision-making of the NES, making the system operation more economical and practical.

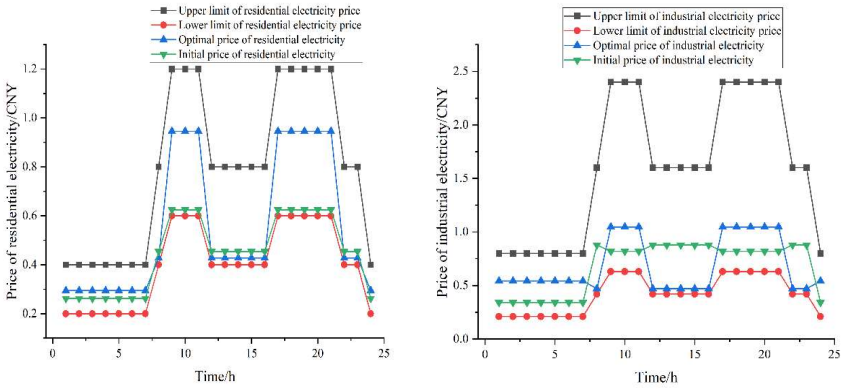

(a) **(b)**

Figure 6. (a) Time of use price of residential electricity; **(b)** and industrial electricity.

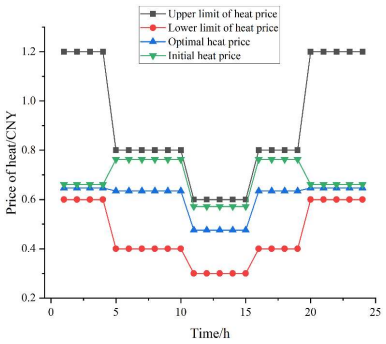

Figure 7. Time of use price of heat energy.

Figure 8 shows the electricity balance of IES. The WT provides electricity at all time periods in a typical day. The PV provides electricity during 6–19 h due to the restriction of sunlight intensity. The ESS is charged at 1–3 h, 9–10 h, 14–15 h, and 24 h, and discharged at 10 h, 12 h, and 17–20 h, which effectively mitigates the waste of power and reduces the cost of purchasing power from the grid. To address the problem of unstable output of new energy, CHP, which is driven by the purified biogas, is applied to provide power for users. The power generated by NES and purchased from the grid is able to meet the demand of BP and the user in this case.

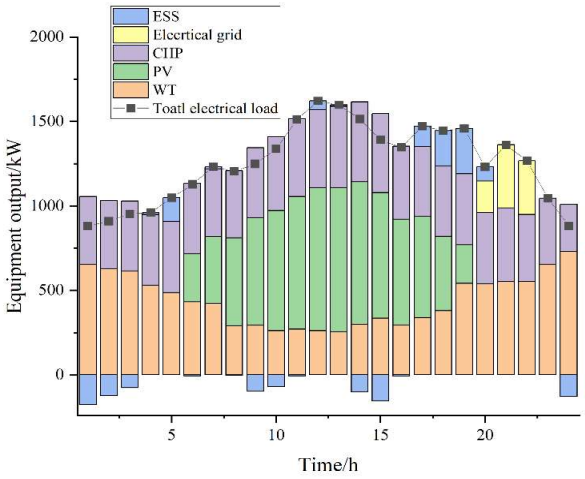

Figure 8. Electricity balance of IES at different time.

The heat balance of IES is shown in **Figure 9**. The heat energy is supplied steadily throughout the whole period by CHP, which satisfies the needs of BP and the user. Moreover, the excess heat energy is provided to the grid for benefits. The biogas boiler has no heat output in 11–15 h due to the lower heat price compared to the cost of the biogas boiler. The shiftable heat load is evenly distributed in 11–13 h, and comparing the time of use heat price in **Figure 7**, it can be found that the heat price set by NES is the lowest in this time period. During the whole time period, the thermal storage tank continuously supplies heat to BP in order to keep the internal temperature of digesters, so the heat loss exists in the whole day.

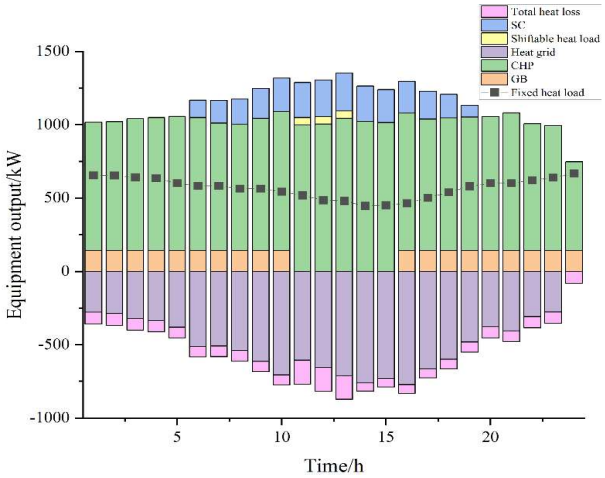

Figure 9. Heat balance of IES at different time.

As can be seen from **Figure 10**, the shiftable electrical load-1, which represents the process of fertilizer crushing, is distributed in 12–14 h, and the shiftable electrical load-2, which stands for the process of solid-liquid separation, is distributed in 21–22 h. The optimization of flexible load distribution

not only results from cost savings but also takes into account the process characteristics in BP. As can be seen in **Figure 10**, the transferable electrical load is unevenly distributed in a typical day. Combined with the residential electricity price, it can be found that the transferable load is larger in flat time and valley time and smaller in peak time. The rearrangement of flexible loads can not only reduce the energy cost but also alleviate the power shortage in peak time, playing the important role of peak shaving and valley filling.

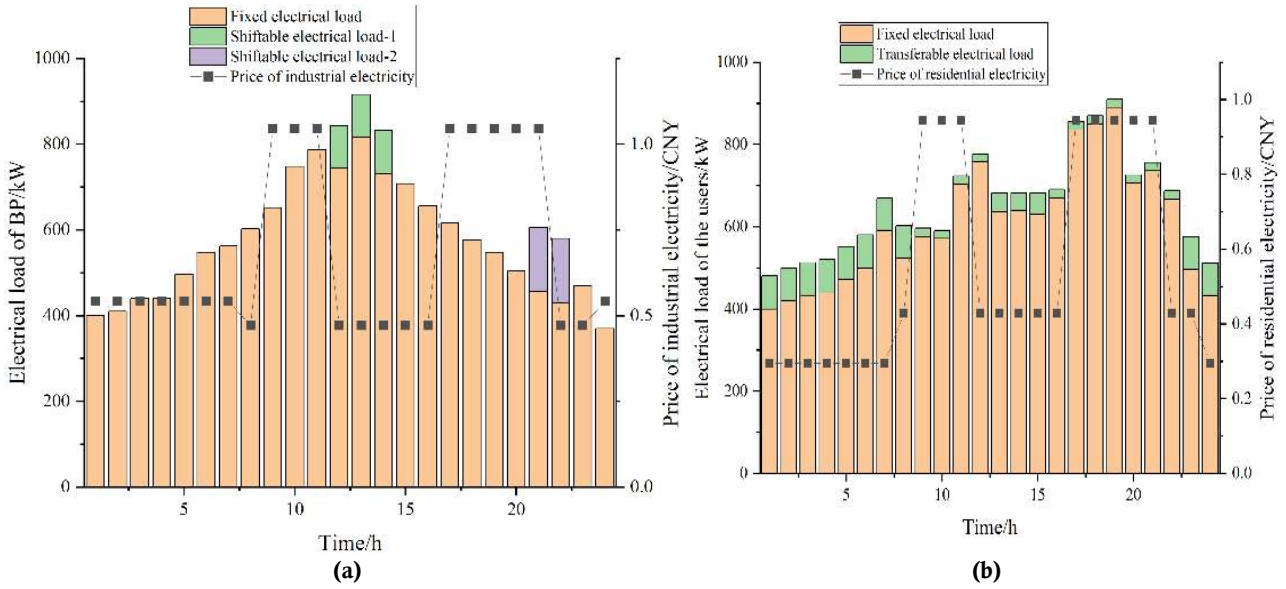

Figure 10. (a) electrical load distribution of BP; and **(b)** the user.

In **Figures 11** and **12**, initial results come from the best individual of the initial generation. As can be seen above, the cost of NES is slightly reduced after optimization, while the total cost of BP obviously decreases by 4.5% in this case. Besides, the profits of NES and BP grow by 5.4% and 4.0% after optimization, respectively. A certain increase in the energy cost of the user can be observed in **Figure 11**, which is the result of a higher electricity price in peak time after optimization. The case results prove that the IES model introduced in this paper is able to improve the profits of leaders and consider the interests of followers, making our game model more applicable for the market.

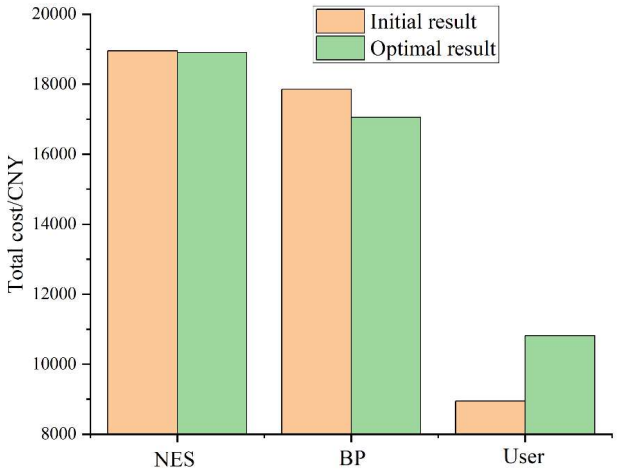

Figure 11. Comparison of total costs of NES, BP and the user.

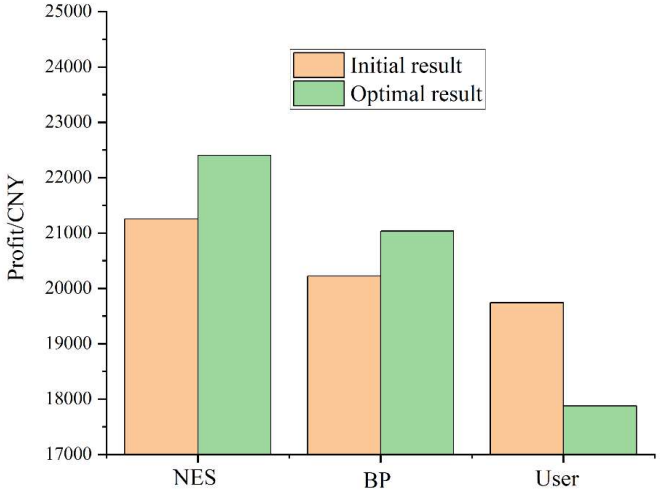

Figure 12. Comparison of profits of NES, BP and the user.

In **Figure 13**, the iteration process and the iteration results of the three different strategies are compared. The composite strategy used in this paper shows similar convergence speed compared to the DE/Best2 strategy, but the fitness value of the composite strategy is noticeably higher than that of the DE/Best2 strategy. This indicates that the DE/Best2 strategy is more likely to fall into a local optimum, while the composite strategy avoids this drawback. Compared with the DE/Rand2 strategy, the composite strategy exhibits significantly faster convergence speed and better fitness values in the iteration process. It demonstrates that our composite strategy has both stronger global-searching ability and local-searching ability compared to the traditional mutation strategy, leading to shorter convergence times and better equilibrium solutions.

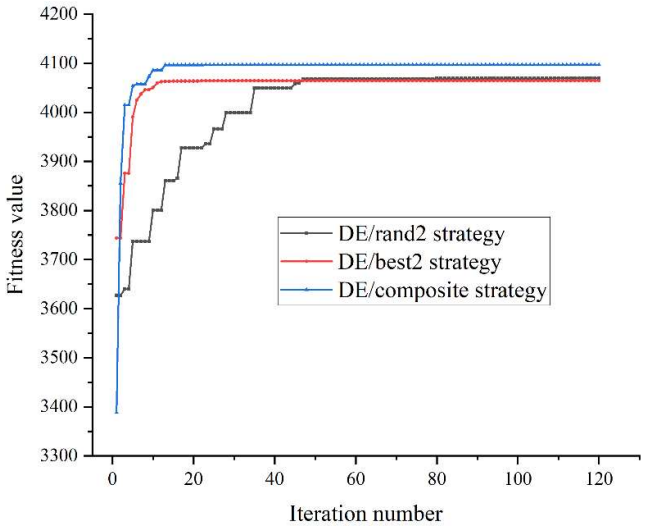

Figure 13. Comparison of best fitness value of three strategies in iteration.

4. Conclusion

This paper constructs a muti-participant Stackelberg game model for rural integrated energy systems (IES), where the interests of the leader and follower are both considered. The profit of NES is increased by 5.4% and the cost of BP is decreased by 4.5% after optimization, proving that our Stackelberg game-based IES is able to balance the interests between the leader and follower. Moreover, we develop an improved differential evolutionary algorithm (DEA) to solve the Stackelberg game. As a comparison, our

improved DEA shows much higher convergence speed than the algorithm using the DE/rand2 strategy and exhibits better equilibrium solutions than the DE/best2 strategy. The conclusions are summarized hereafter:

(1) In 2022, industrial electricity accounts for 67% of the national electricity consumption in China; thus, industrial users are a significant participant in the electricity market. In this study, industrial users—biogas plants—are first introduced into IES, and the load of BP is divided into different types of flexible loads according to their process characteristics so that they can participate in the Stackelberg game together with common users. The game model and solution method in our study provide reliable and practical reference information for electricity industry participants so that they can find better methods to coordinate relationships between energy suppliers, industrial users, and the common user.

(2) This paper establishes an improved DEA to solve the Stackelberg game with multiple participants and multiple variables, which has faster convergence speed and better equilibrium results than traditional DEA, markedly reducing the computational cost of the model. Moreover, our improved DEA provides ideas for the development of new algorithms. Applying different mutation methods at different stages under the control of a specific operator can effectively combine the advantages of different methods and avoid their disadvantages.

(3) In previous studies, most results of the Stackelberg game-based model focused on increasing the benefit of the leader but ignored the benefit of other players. However, the Stackelberg game result in this paper not only improves the leader's profit but also takes into account the interests of the followers, avoiding the situation of "single winner" in the traditional game model. The game result of our model can be a meaningful sample for decision-makers in the electricity market to balance interests between different stakeholders, showing more practical value and reference significance.

As the trend of interactive behaviors in the energy market becomes more and more obvious, the Stackelberg game-based IES proposed in this paper can help to analyze the interaction process between different decision-making bodies and find the optimal equilibrium strategy, which can provide important reference information for decision-makers in the market and the government.

Author contributions

Conceptualization, TL and YG; methodology, YG; software, TL; validation, TL and YG; formal analysis, TL; investigation, TL; resources, YG; data curation, TL; writing—original draft preparation, TL; writing—review and editing, YG; visualization, TL; supervision, YG; project administration, YG; funding acquisition, YG. All authors have read and agreed to the published version of the manuscript.

Conflict of interest

The authors declare no conflict of interest.

Abbreviations

IES	Integrated energy system	$P^{e}_{CHP,t}$	Electrical energy produced by CHP at time t
NES	New energy supplier	$P^{g}_{CHP,t}$	Gas consumption of CHP at time t
BP	Biogas plant	$P^{h}_{CHP,t}$	Heat power produced by WHB at time t
DEA	Differential evolutionary algorithm	$P^{e}_{CHP,max}$	Rated power of CHP
WT	Wind turbines	$E_{ESS,t}$	Electric power stored by ESS at time t

PV	Photovoltaic panels
CHP	Combined heat and power
ESS	Energy storage system
GB	Gas boilers
SC	Solar collectors
TST	Thermal storage tanks
CSI	Consumer satisfaction index
WHB	Waste heat boiler
Parameters	
N	Number of participants
ρ_{NES}	Price strategy set by NES
δ_{BP}	Load demand of BP
δ_{user}	Load demand of the user
F_{NES}	Revenue of NES
F_{BP}	Revenue of the biogas plant
F_{user}	Consumer surplus of the user
$F_{\mathrm{NES\text{-}r}}$	Total revenue of NES
$F_{\mathrm{NES\text{-}c}}$	Fuel cost of NES
$F_{\mathrm{NES\text{-}o}}$	Operation cost of equipment of NES
$I_{\mathrm{net},t}$	Electricity grid cost
$I_{\mathrm{sell\text{-}BP},t}$	Revenue derived from BP
$I_{\mathrm{sell\text{-}user},t}$	Revenue derived from user
$G_{\mathrm{CHP},t}$	Amount of biogas used by CHP
$C_{\mathrm{CHP},t}$	Operating cost for CHP at time t
$C_{\mathrm{WT},t}$	Operation cost of WT at time t
$C_{\mathrm{PV},t}$	Operation cost of PV at time t
$C_{\mathrm{ESS},t}$	Operating cost for ESS at time t
$P_{\mathrm{BP},t}$	Electric power sold by NES to BP at time t
$H_{\mathrm{BP},t}$	Heat power sold by NES to BP at time t
$P_{\mathrm{user},t}$	Electric power sold by NES to user at time t
$H_{\mathrm{user},t}$	Heat power sold by NES to user
$p_{\mathrm{buy},t}$	Price of electricity purchased from grid
$p_{\mathrm{sell},t}$	Price of electricity sold to grid
$P_{\mathrm{buy},t}$	Electric power purchased from grid
$P_{\mathrm{sell},t}$	Electric power sold to grid
$P_{\mathrm{device},t}$	Output power of device at time t
$P_{\mathrm{e\text{-}net},t}$	Electric power exchanged with grid at time t
$P_{\mathrm{WT},t}$	Electric power provided by WT at time

$P_{\mathrm{ESS},t}$	Charging and discharging power at time t
$P_{\mathrm{max},t}$	Maximum charging and discharging ability of ESS
$F_{\mathrm{BP\text{-}r}}$	Total revenue of BP
$F_{\mathrm{BP\text{-}c}}$	Energy cost of BP
$F_{\mathrm{BP\text{-}o}}$	Operating cost of equipment in BP
$I^{\mathrm{g}}_{\mathrm{sell},t}$	Revenue generated from selling biogas
$I^{\mathrm{OF}}_{\mathrm{sell},t}$	Revenue generated from selling organic fertilizer
$C_{\mathrm{e},t}$	Cost of purchasing electricity of BP from NES
$C_{\mathrm{h},t}$	Cost of purchasing heat of BP from NES
$C_{\mathrm{SC},t}$	Operating cost of solar collector at time t
$C_{\mathrm{GB},t}$	Operating cost of biogas boiler
$P_{\mathrm{BP,fix}}$	Fixed electrical load of BP
$P_{\mathrm{BP,shift1}}$	Shiftable electrical load of crushing process
$P_{\mathrm{BP,shift2}}$	Shiftable electrical load of solid-liquid separation process
τ_1/τ_2	Starting time of shiftable loads
t_{shift1}	Total operating hours of crushing process
t_{shift2}	Total operating hours of solid-liquid separation process
$y_{\mathrm{h1}}/y_{\mathrm{h2}}$	State variable that determines whether or not load has been shifted
h_{shift}	Total operating hours of drying process
$H^{\mathrm{fix}}_{\mathrm{BP}}$	Fixed heat load
$H^{\mathrm{shift}}_{\mathrm{BP}}$	Shiftable heat load
$H^{\mathrm{fix}}_{\mathrm{GB},t}$	Heat power produced by GB for fixed heat load at time t
$H^{\mathrm{fix}}_{\mathrm{CHP},t}$	Heat power produced by CHP for fixed heat load at time t
$H_{\mathrm{SC},t}$	Heat power generated by solar collector at time t
$H_{\mathrm{loss},t}$	Total heat loss of TST at time t
$H_{\mathrm{tank},t}$	Heat power received by TST at time t
$H_{\mathrm{wa\text{-}loss}}$	Decrease of heat caused by circulating water
$H_{\mathrm{tank\text{-}loss}}$	Heat loss through metal tank
$H^{\mathrm{sft}}_{\mathrm{GB},t}$	Heat power produced by GB for shiftable heat load at time t
$H^{\mathrm{sft}}_{\mathrm{CHP},t}$	Heat power produced by CHP for shiftable heat load at time t
$H_{\mathrm{buy},t}$	Total heat energy BP purchased from NES
H_{out}	Heat of circulating water output from TST
H_{in}	Heat of circulating water input to TST
G_{BP}	Daily biogas production of BP
G_{OF}	Daily production of organic fertilizer
R_{OF}	Organic fertilizer content of biogas residue
P_{OF}	Total electricity consumed by fertilizer production process
G_{T}	Solar flux received by SC

	t		
$P_{PV,t}$	Electric power provided by PV at time t	$H_{GB,t}$	Heat power production of GB at time t
$P_{CHP,t}$	Electric power provided by CHP at time t	$G_{GB,t}$	Gas consumption of GB at time t
$P^{ch}_{ESS,t}$	Charging power of storage system	U	Consumer satisfaction index
$P^{dis}_{ESS,t}$	Discharging power of storage system	$I^{e}_{buy,t}$/ $I^{h}_{buy,t}$/ $I^{g}_{buy,t}$	Costs of purchasing electricity, heat and biogas
$H_{CHP,t}$	Heat power produced by CHP at time t	ω	Parameter representing user's preference
$H_{net,t}$	Heat power sold to heat grid at time t	P_{trans}	Transferred load power
$V_{cut,i}$	Cut-in wind speeds	$Z_{j,k}$	j-th chaotic variable in population
$V_{cut,o}$	Cut-out wind speeds	F_t	Fitness function

References

1. Zhu G, Gao Y, Sun H. Optimization scheduling of a wind–photovoltaic–gas–electric vehicles Community-Integrated Energy System considering uncertainty and carbon emissions reduction. Sustainable Energy, Grids and Networks. 2023; 33: 100973. doi: 10.1016/j.segan.2022.100973
2. Lu Z, Gao Y, Xu C. Evaluation of energy management system for regional integrated energy system under interval type-2 hesitant fuzzy environment. Energy. 2021; 222: 119860. doi: 10.1016/j.energy.2021.119860
3. Escribano G, González-Enríquez C, Lázaro-Touza L, et al. An energy union without interconnections? Public acceptance of cross-border interconnectors in four European countries. Energy. 2023; 266: 126385. doi: 10.1016/j.energy.2022.126385
4. Wu D, Han Z, Liu Z, et al. Comparative study of optimization method and optimal operation strategy for multi-scenario integrated energy system. Energy. 2021; 217: 119311. doi: 10.1016/j.energy.2020.119311
5. Cano PI, Almenglo F, Ramírez M, et al. Integration of a nitrification bioreactor and an anoxic biotrickling filter for simultaneous ammonium-rich water treatment and biogas desulfurization. Chemosphere. 2021; 284: 131358. doi: 10.1016/j.chemosphere.2021.131358
6. Wang Y, Guo L, Ma Y, et al. Study on operation optimization of decentralized integrated energy system in northern rural areas based on multi-objective. Energy Reports. 2022; 8: 3063-3084. doi: 10.1016/j.egyr.2022.01.246
7. Tan H, Li Z, Wang Q, et al. A novel forecast scenario-based robust energy management method for integrated rural energy systems with greenhouses. Applied Energy. 2023; 330: 120343. doi: 10.1016/j.apenergy.2022.120343
8. Jiang Q, Mu Y, Jia H, et al. A Stackelberg Game-based planning approach for integrated community energy system considering multiple participants. Energy. 2022; 258: 124802. doi: 10.1016/j.energy.2022.124802
9. Wang Y, Liu Z, Wang J, et al. A Stackelberg game-based approach to transaction optimization for distributed integrated energy system. Energy. 2023; 283: 128475. doi: 10.1016/j.energy.2023.128475
10. Jiang H, Ning S, Ge Q, et al. Optimal economic dispatching of multi‐microgrids by an improved genetic algorithm. IET Cyber-Systems and Robotics. 2021; 3(1): 68-76. doi: 10.1049/csy2.12008
11. Youssef H, Kamel S, Hassan MH, et al. Optimizing energy consumption patterns of smart home using a developed elite evolutionary strategy artificial ecosystem optimization algorithm. Energy. 2023; 278: 127793. doi: 10.1016/j.energy.2023.127793
12. Enhancing biogas generation from lignocellulosic biomass through biological pretreatment: Exploring the role of ruminant microbes and anaerobic fungi—ScienceDirect [EB/OL]. Available online: https://www.sciencedirect.com/science/article/pii/S1075996423001282 (accessed on 7 January 2024).
13. Demirci A, Akar O, Ozturk Z. Technical-environmental-economic evaluation of biomass-based hybrid power system with energy storage for rural electrification. Renewable Energy. 2022; 195: 1202-1217. doi: 10.1016/j.renene.2022.06.097
14. Fu X, Zhou Y. Collaborative Optimization of PV Greenhouses and Clean Energy Systems in Rural Areas. IEEE Transactions on Sustainable Energy. 2023; 14(1): 642-656. doi: 10.1109/tste.2022.3223684
15. Qin M, Yang Y, Chen S, et al. Bi-level optimization model of integrated biogas energy system considering the thermal comfort of heat customers and the price fluctuation of natural gas. International Journal of Electrical Power & Energy Systems. 2023; 151: 109168. doi: 10.1016/j.ijepes.2023.109168
16. Wang L, Yang R, Qu Y, et al. Stackelberg game-based optimal scheduling of integrated energy systems

considering differences in heat demand across multi-functional areas. Energy Reports. 2022; 8: 11885-11898. doi: 10.1016/j.egyr.2022.08.199
17. Yuan G, Gao Y, Ye B. Optimal dispatching strategy and real-time pricing for multi-regional integrated energy systems based on demand response. Renewable Energy. 2021; 179: 1424-1446. doi: 10.1016/j.renene.2021.07.036
18. Huang Y, Wang Y, Liu N. A two-stage energy management for heat-electricity integrated energy system considering dynamic pricing of Stackelberg game and operation strategy optimization. Energy. 2022; 244: 122576. doi: 10.1016/j.energy.2021.122576
19. Li P, Wang Z, Yang W, et al. Hierarchically partitioned coordinated operation of distributed integrated energy system based on a master-slave game. Energy. 2021; 214: 119006. doi: 10.1016/j.energy.2020.119006
20. Wang Y, Cai C, Liu C, et al. Planning research on rural integrated energy system based on coupled utilization of biomass-solar energy resources. Sustainable Energy Technologies and Assessments. 2022; 53: 102416. doi: 10.1016/j.seta.2022.102416
21. Zhang Z, Chica M, Tang Q, et al. A multi-objective co-evolutionary algorithm for energy and cost-oriented mixed-model assembly line balancing with multi-skilled workers. Expert Systems with Applications. 2024; 236: 121221. doi: 10.1016/j.eswa.2023.121221
22. Deep S, Sarkar A, Ghawat M, et al. Estimation of the wind energy potential for coastal locations in India using the Weibull model. Renewable Energy. 2020; 161: 319-339. doi: 10.1016/j.renene.2020.07.054
23. Yang D, Wang M, Yang R, et al. Optimal dispatching of an energy system with integrated compressed air energy storage and demand response. Energy. 2021; 234: 121232. doi: 10.1016/j.energy.2021.121232
24. Chen Z, Yiliang X, Hongxia Z, et al. Optimal design and performance assessment for a solar powered electricity, heating and hydrogen integrated energy system. Energy. 2023; 262: 125453. doi: 10.1016/j.energy.2022.125453
25. Wang Y, Wen X, Gu B, et al. Power Scheduling Optimization Method of Wind-Hydrogen Integrated Energy System Based on the Improved AUKF Algorithm. Mathematics. 2022; 10(22): 4207. doi: 10.3390/math10224207
26. Javed MS, Jurasz J, McPherson M, et al. Quantitative evaluation of renewable-energy-based remote microgrids: curtailment, load shifting, and reliability. Renewable and Sustainable Energy Reviews. 2022; 164: 112516. doi: 10.1016/j.rser.2022.112516
27. Luo Y, Gao Y, Fan D. Real-time demand response strategy base on price and incentive considering multi-energy in smart grid: A bi-level optimization method. International Journal of Electrical Power & Energy Systems. 2023; 153: 109354. doi: 10.1016/j.ijepes.2023.109354
28. Zhu G, Gao Y. Multi-objective optimal scheduling of an integrated energy system under the multi-time scale ladder-type carbon trading mechanism. Journal of Cleaner Production. 2023; 417: 137922. doi: 10.1016/j.jclepro.2023.137922